sustainable chemistry

MDPI

Review

High-Temperature Stability of $LiFePO_4$/Carbon Lithium-Ion Batteries: Challenges and Strategies

Guangyao Jin, Wanwei Zhao, Jianing Zhang, Wenyu Liang *, Mingyang Chen * and Rui Xu *

School of Materials Science and Engineering, University of Science and Technology Beijing, Beijing 100083, China
* Correspondence: liangw@ustb.edu.cn (W.L.); mychen@ustb.edu.cn (M.C.); ruixu@ustb.edu.cn (R.X.)

Abstract: Lithium-ion batteries that use lithium iron phosphate ($LiFePO_4$) as the cathode material and carbon (graphite or MCMB) as the anode have gained significant attention due to their cost-effectiveness, low environmental impact, and strong safety profile. These advantages make them suitable for a wide range of applications including electric vehicles, stationary energy storage, and backup power systems. However, their adoption is hindered by a critical challenge: capacity degradation at elevated temperatures. This review systematically summarizes the corresponding modification strategies including surface modification of the anode and cathode as well as modification of the electrolyte, separator, binder, and collector. We further discuss the control of the charge state, early warning prevention, control of thermal runaway, and the rational application of ML and DFT to enhance the LFP/C high temperature cycling stability. Finally, in light of the current research challenges, promising research directions are presented, aiming at enhancing their performance and stability in such harsh thermal environments.

Keywords: $LiFePO_4$; high-temperature stability; degradation mechanisms; modification strategies

Academic Editors: Francesca Deganello and Jan-Willem Bos

Received: 20 December 2024
Revised: 12 February 2025
Accepted: 20 February 2025
Published: 27 February 2025

Citation: Jin, G.; Zhao, W.; Zhang, J.; Liang, W.; Chen, M.; Xu, R. High-Temperature Stability of $LiFePO_4$/Carbon Lithium-Ion Batteries: Challenges and Strategies. *Sustain. Chem.* **2025**, *6*, 7. https://doi.org/10.3390/suschem6010007

1. Introduction

Lithium iron phosphate batteries ($LiFePO_4$) have emerged as a promising contender in the realm of commercial lithium-ion batteries (LIBs). These batteries employ $LiFePO_4$ as the cathode material and carbon (graphite or mesocarbon microbeads (MCMBs)) as the conventional anode. Despite having a lower operating potential (approximately 3.4 V) compared with other high-energy-density cathodes, like Ni-rich layered oxides ($LiNi_xMn_yCo_{1-x-y}O_2$, approximately 3.8 V), $LiFePO_4$ batteries possess a unique set of advantages including low cost, low toxicity, low self-discharge, long cycle life, high power capabilities, and remarkable thermal stability [1–12]. As a result, they have found applications in electric vehicles (EVs), utility-scale stationary energy storage, and backup power systems. Nonetheless, $LiFePO_4$/carbon secondary batteries confront an inherent challenge—rapid capacity degradation under elevated temperatures, presenting a notable impediment to their widespread adoption, especially in the context of electric vehicles. Large batteries, employed in electric vehicles and hybrid electric vehicles (EVs/HEVs), frequently encounter elevated internal temperatures during operation, even in typical environmental conditions. For instance, during EV/HEV operation at usual ambient temperatures, LIBs can reach internal temperatures exceeding 60 °C, with even higher electrolyte temperatures. This issue is further exacerbated by high-pulse cycling in high-power batteries such as those used in EVs and HEVs [13,14]. Electric vehicles are also subjected to extreme temperature fluctuations, ranging from −40 °C to 70 °C, coupled with high charge and discharge rates, collectively

contributing to elevated temperatures [15]. Consequently, the performance criteria for LIBs in high-temperature conditions are stringent.

Understanding the degradation mechanisms of $LiFePO_4$-based batteries under high-temperature conditions is paramount to the development of effective modification strategies. Researchers have extensively delved into the behavior of $LiFePO_4$ cathode materials, electrolytes, and other battery components when subjected to elevated temperatures. The primary cause of severe capacity decay at elevated temperatures is the dissolution of Fe^{2+} ions from the cathode to the electrolyte and its deposition on the anode, hindering the intercalation of Li^+ ions and leading to the formation of a thick and irreversible solid electrolyte interface (SEI) layer. Commonly used electrolytes, like lithium hexafluorophosphate ($LiPF_6$) dissolved in a carbonate-based organic solvent, are susceptible to thermal decomposition, producing acidic substances that corrode the anode and active cathode materials. Additionally, the side reactions between the electrolyte and the anode as well as significant structural changes in both $LiFePO_4$ and carbon anode materials at very high or very low state-of-charge (SOC) ranges contribute to high impedance polarization and thick SEI formation.

Building on these mechanistic insights, a diverse range of modification strategies has been crafted to bolster the stability and performance of $LiFePO_4$-based batteries in high-temperature environments. Cathode protective strategies such as coatings, doping, and producing composite materials could effectively mitigate iron dissolution. Coating the anode with Au or Cu metals could effectively absorb the dissolved Fe and prevent electrode-electrolyte side reactions, improving stability. The replacement of the electrolyte or the adoption of additives, such as LiTFSI, LiBOB, LiODFB, or vinylene carbonate (VC), has been successful in reducing Fe dissolution and electrolyte decomposition, and consequently improving the $LiFePO_4$ battery's high-temperature stability. Furthermore, optimizing operating conditions, particularly SOC control, is paramount in determining the performance and longevity of $LiFePO_4$-based LIBs.

In this comprehensive review, we consolidate the research findings related to the degradation mechanisms of $LiFePO_4$-based LIBs. Additionally, we provide a detailed discussion on diverse strategies and modifications aimed at improving high-temperature performance.

2. Basic Characteristics of $LiFePO_4$/Carbon Batteries

2.1. $LiFePO_4$ Cathode Material

Compared with conventional cathode materials like $LiCoO_2$, $LiNiO_2$, and $LiMn_2O_4$, $LiFePO_4$ boasts several advantages including significant theoretical capacity (approximately 170 mAh g^{-1}), a moderate operating voltage plateau (the Fe^{3+}/Fe^{2+} redox couple conveniently located at 3.4 V versus Li^+/Li, compatible with common organic and polymer electrolytes), and a theoretical energy density of 580 Wh kg^{-1} versus Li^+/Li, surpassing that of $LiCoO_2$. $LiFePO_4$ is also known for its thermal stability, excellent reversibility, cost-effectiveness, and environmental friendliness [16].

$LiFePO_4$, belonging to the olivine family of cathode materials, exhibits an orthorhombic lattice structure within the Pnma space group [17]. Its lattice structure features oxygen atoms arranged in a slightly distorted hexagonal-close-packed configuration. Within this structure, phosphorus atoms occupy tetrahedral sites, while iron and lithium atoms reside in the octahedral 4a and 4c sites, respectively. In this crystalline matrix, each FeO_6 octahedron forms interconnected zigzag planes through common corners in the b–c plane. Simultaneously, LiO_6 octahedra create edge-sharing chains along the b-axis, with one FeO_6 octahedron sharing edges with two LiO_6 octahedra. Furthermore, PO_4 groups share one edge with an FeO_6 octahedron and two edges with LiO_6 octahedra, as illustrated

in Figure 1. Due to its structural characteristics, $LiFePO_4$ demonstrates an exceptional stability during electrochemical charge and discharge operations at ambient temperature. Its volume change content during delithiation is a mere 6.81%, which effectively prevents capacity degradation associated with volume fluctuations over extended cycles [8]. This, coupled with the strong P–O covalent bonds, results in excellent thermal stability, cyclability, and safety.

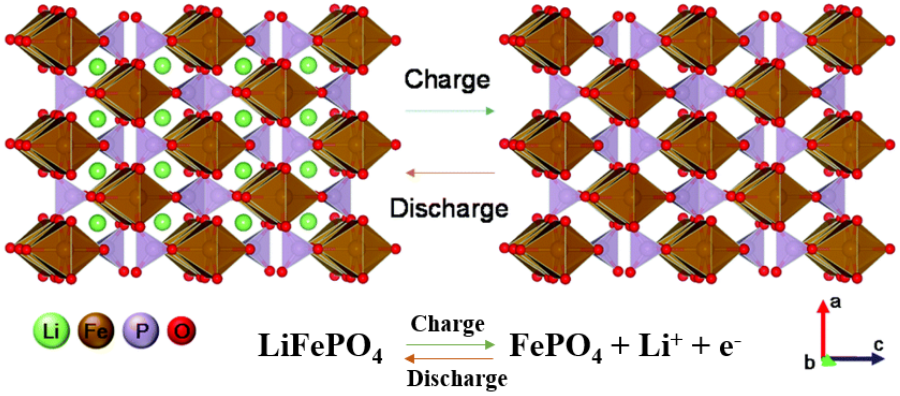

Figure 1. Crystal structures of $LiFePO_4$ and $FePO_4$. During charging, $LiFePO_4$ changes to $FePO_4$ by delithiation. In the discharge process, a reversible transformation from $FePO_4$ to $LiFePO_4$ occurs by lithiation. The image was taken with permission [8].

However, it is important to note several intrinsic limitations of this olivine-type cathode material for LIBs. First, $LiFePO_4$ exhibits low intrinsic electronic conductivity, measuring less than 10^{-8} S cm^{-1}, which hinders the full utilization of its theoretical capacity. Second, it has a low Li-ion diffusion coefficient, with chemical diffusion coefficients ranging from 10^{-14} to 10^{-16} cm^2 s^{-1}, dependent on the Li concentration and characterization method used [18]. These intrinsic deficiencies in $LiFePO_4$ narrow the acceptable working temperature range of $LiFePO_4$ batteries. Operating beyond the moderate temperature zone can lead to rapid capacity fade and safety risks including the potential for fire and explosion, thereby limiting the commercial viability of such batteries.

2.2. Carbon Anode Materials

Graphite as the anode material: Graphite has been widely adopted as an anode material for the past two decades due to its safety and environmental friendliness. As seen in Figure 2, graphite has a layered structure [19], and it offers several advantages including cost-effectiveness, ease of preparation, and versatility in various forms. Graphite operates through a lithium-ion insertion/extraction mechanism during the charge/discharge process. As Li^+ undergoes intercalation into graphite carbon to form LiC_6, it provides a specific capacity of 372 mAh g^{-1} [20]. While this capacity for an anode may not be exceptionally high, ongoing research into next-generation anode materials such as silicon is underway. However, it is important to note that, at present, graphite remains the most extensively utilized anode material for commercial LIBs.

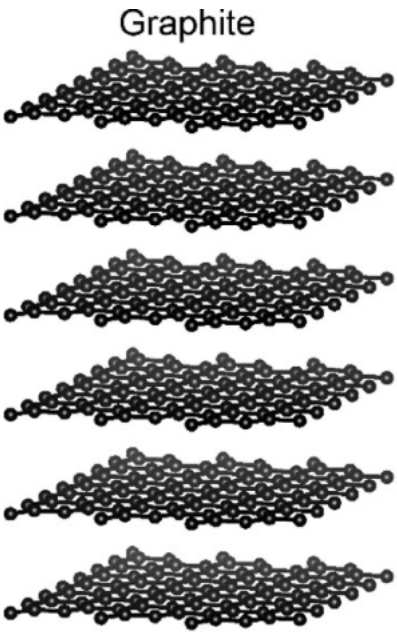

Figure 2. The structure of graphite. The image was taken with permission [19].

At elevated temperatures, it has been observed that the growth of the SEI layer on the surface of the graphite electrode accelerates. This acceleration may lead to lithium immobilization in the SEI layers and hinder the accessibility of Li^+ to the graphite electrode [21]. The heightened SEI growth is suspected to be associated with the dissolution of iron from the cathode and the deposition on the anode, which is minimal at moderate temperatures but becomes more pronounced at elevated temperatures. The blocking of the graphite electrode by the SEI layer can ultimately result in a decrease in the anode's storage capacity, as it impedes the intercalation of lithium.

MCMB as the anode material: Mesocarbon microbeads (MCMBs) are a standout carbon material for lithium-ion batteries (LIBs) due to their distinctive attributes. Produced via the heat treatment of coal tar or coal tar pitch, MCMBs polymerize polyaromatic hydrocarbon molecules, resulting in an ordered structure despite the initial pitch disorder. Figure 3 shows the structure of MCMBs [22], and their regular spherical shape (1 to 40 μm) and close-packed arrangement contribute to a high volumetric energy density. The ordered lamellar structure and low surface area of MCMBs enhance cycle life and electrical conductivity at low voltage, making MCMBs advantageous [21,23–26]. MCMBs' electrochemical performance aligns with its carbon microstructure design. MCMBs with numerous micropores or increased carbon layer spacing facilitate faster Li^+ migration, improving the charge and discharge capacity and rate performance. Conversely, smaller particle sizes enhance the rate performance but may reduce the reversible capacity and charge–discharge efficiency due to increased electrode surface area and thus more SEI growth.

Despite the advantages of MCMBs, such as Li^+ dispersion and mechanical stability, its low theoretical specific capacity poses a developmental challenge. Hence, ongoing research has focused on modifying MCMBs and their composites for improved performance. At elevated temperatures, while the MCMBs themselves remain stable, it can still be a primary factor contributing to the performance degradation of a $LiFePO_4$/MCMB battery. This is attributed to the increased growth of the SEI layer, similar to that observed in a graphite anode, which impedes the accessibility of Li^+ ions to the graphite electrode.

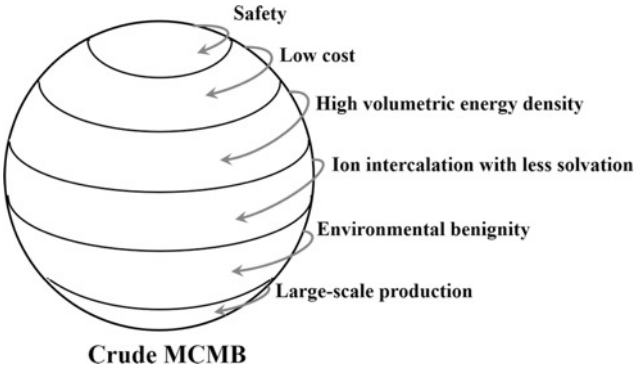

Figure 3. The structures of MCMBs. The image was taken with permission [22].

2.3. Major Electrolytes and Electrode–Electrolyte Interface Characteristics in $LiFePO_4$/Carbon Batteries

The most commonly used electrolyte for $LiFePO_4$-based batteries comprises $LiPF_6$ dissolved in a mixture of organic carbonate solvents. Among the prevalent solvents are propylene carbonate (PC), ethylene carbonate (EC), dimethyl carbonate (DMC), and diethyl carbonate (DEC). $LiFePO_4$ electrodes exhibit stability in standard $LiPF_6$ solutions at ambient temperatures. However, challenges emerge when the batteries are exposed to elevated temperatures, specifically around 60 °C [27]. The aging of Li_xFePO_4 cathodes in $LiPF_6$ solutions at 60 °C results in capacity degradation, which can be attributed to Fe dissolution and a significant increase in electrode impedance, leading to sluggish redox reaction kinetics [28].

An alternative conductive salt is lithium bis(oxalato)borate (LiBOB). LiBOB has garnered significant attention in the realm of $LiFePO_4$-based battery salts due to its excellent thermal stability, boasting a decomposition temperature exceeding 290 °C [29]. However, LiBOB does exhibit some limitations, primarily its solubility in solvents such as EC and PC, which restricts the concentration of LiBOB that can be effectively utilized (typically < 1 M, dependent on the solvents employed). Another noteworthy lithium salt is lithium oxalyldifluoroborate (LiODFB). This compound features a structural variation from LiBOB, where one oxalato group is replaced by two fluorine groups. LiODFB combines properties from both LiBOB and lithium tetrafluoroborate ($LiBF_4$), offering enhanced solubility compared with LiBOB, thereby allowing for higher concentrations of the salt. Consequently, the conductivity of LiODFB is improved compared with LiBOB, and it is on par with that of $LiPF_6$. Previous studies have effectively demonstrated that LiODFB retains a much higher capacity (88% after 100 cycles) compared with $LiPF_6$ (50% after 100 cycles) when cycled at 65 °C in $LiFePO_4$/graphite full cells [30].

3. Primary Factors Contributing to Performance Degradation in $LiFePO_4$/Carbon Batteries During High-Temperature Application

$LiFePO_4$/C batteries operated within a moderate temperature range exhibit exceptional reversibility with negligible capacity decay under standard operating conditions. However, commercial lithium ion batteries commonly encounter challenges related to high-temperature environments. In the case of large-scale LIBs engaged in rapid charge and discharge cycles, there is a rapid increase in temperature, further elevating the battery's operating temperature. When subject to elevated temperatures, $LiFePO_4$/carbon batteries are susceptible to rapid capacity deterioration. Although $LiFePO_4$ maintains a relatively low operating potential compared with other cathode materials in LIBs (such as layered oxide-based cathodes), thus mitigating the problem of electrolyte oxidation when operated at elevated temperatures, there is still a concern. The dissolution of Fe^{2+} ions from the $LiFePO_4$ cathode into the electrolyte can lead to a minor loss of active materials from the

cathode. Even more concerning is the potential for these Fe^{2+} ions to undergo reduction on the anode surface, which subsequently deteriorates the SEI. This leads to elevated internal resistance and a decrease in the available Li inventory, ultimately contributing to further capacity degradation in the battery.

3.1. Anode Side

In $LiFePO_4$-based batteries, particularly during high-temperature storage, capacity degradation is primarily driven by the consumption of active lithium in conjunction with the evolution of the SEI film on the anode (see Figure 4) [31–33]. Studies suggest that elevated temperatures exacerbate the decomposition of the SEI film, leading to its continuous regeneration, which significantly consumes active lithium. This mechanism remains a major contributor to accelerated capacity fade [32,34].

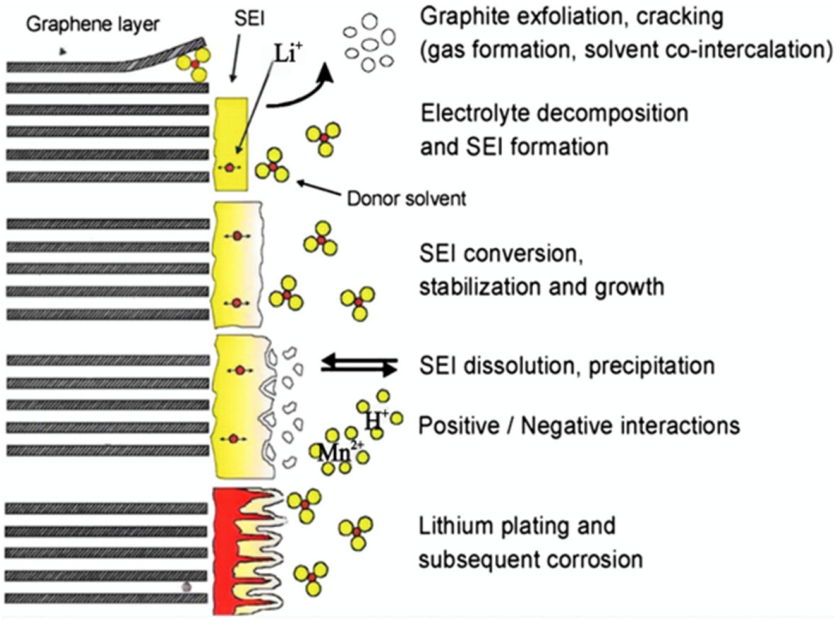

Figure 4. Schematic diagram of SEI degradation pattern on the graphite anode side of the LFP cell. The image was taken with permission [33].

Several studies have delved into the degradation mechanisms of $LiFePO_4$ batteries under elevated temperatures. For instance, Kassem et al. [35] conducted post-mortem analyses on eight Ah $LiFePO_4$/graphite commercial batteries stored at varying temperatures and SOC. They observed that elevated temperatures and high SOC levels exacerbated the decomposition and regeneration of the SEI film on the graphite anode. Significantly, the change in anode impedance was more pronounced than that of the cathode, with active lithium consumption emerging as the primary driver of battery degradation. Similarly, Lewerenz et al. [36] conducted cyclic tests on eight Ah $LiFePO_4$/graphite cells at 40 °C. Detailed analysis of the covering layer on the anode's surface following cyclic aging unveiled a composition that included plated active lithium, deposited iron, and the SEI film. The dissolution of Fe from the cathode was attributed to the elevated temperature. In the later stages of aging, segments of the anode became deactivated due to limited Li^+ ion conductivity. This led to an accelerated capacity decline and a noticeable increase in internal resistance.

3.2. Cathode Side

At standard ambient temperatures, the $LiFePO_4$ cathode is known for its stability and reliability, distinguishing it from many other LIB cathodes. However, at elevated temperatures, the dissolution of Fe^{2+} ions becomes evident and is recognized as a contributing factor to accelerated capacity loss [32,34].

Considerable research efforts have been dedicated to studying the mechanism of Fe dissolution in $LiFePO_4$ batteries and its effects on cell performance and capacity loss. Substantial progress has been achieved. Initially, only dissolved Fe in the electrolytes of $LiFePO_4$/graphite cells could be detected. However, examinations of graphite-based anode using energy-dispersive X-ray spectroscopy revealed no detectable iron deposits [37]. Later, many studies consistently showed that Fe deposition on the anode led to battery capacity degradation. Lai et al. [38] and Iltchev et al. [39] investigated the impact of Fe^{2+} dissolution in the electrolyte on cell performance. Their findings pointed to the reduction of Fe^{2+} on the surface of the anode, resulting in expedited electrolyte decomposition and the obstruction of the reversible intercalation of Li^+ ions into the graphite electrode. Amine et al. [40] also illustrated a strong correlation between the dissolution, deposition, and possible reduction of Fe^{2+} on the anode's surface and capacity loss. Ongoing electrolyte decomposition occurs on the deposited metallic iron, resulting in heightened cell impedance and reduced capacity retention. Komaba et al. [41] revealed that Fe^{2+} ions were electrochemically reduced on the graphite anode during discharge, creating metal deposits that impede lithium ion intercalation into the graphite and, in some instances, expedite electrolyte decomposition, resulting in the formation of a thick SEI layer. The schematic diagram of iron dissolution is shown in Figure 5 [42]. Striebel et al. corroborated these findings but detected iron oxide deposits rather than metallic iron on the anode's surface [43]. Zaghib et al. proposed another dissolution mechanism, linking Fe dissolution to Fe oxide impurities in $LiFePO_4$ [44].

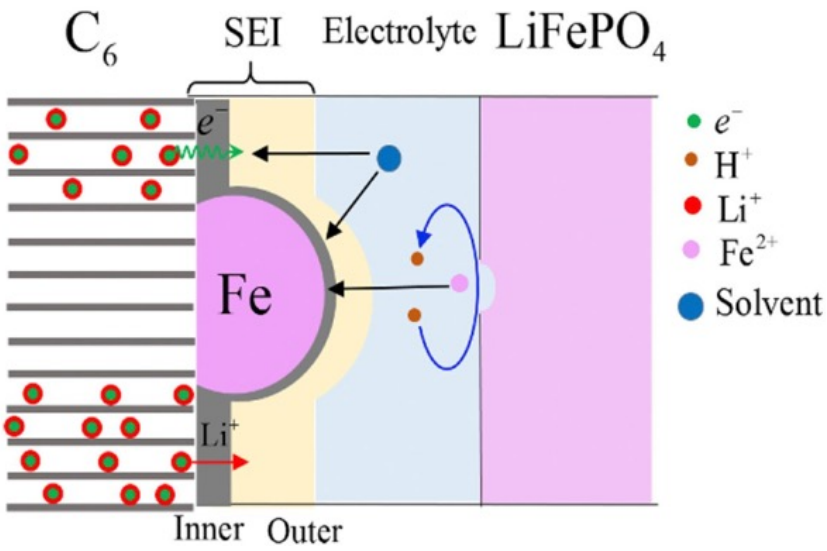

Figure 5. Schematic of LFP cathode iron dissolution. The image was taken with permission [42].

Iron dissolution was primarily attributed to an ion exchange reaction between the iron in $LiFePO_4$ and protons from the formation of HF in organic solvent-based electrolytes containing $LiPF_6$ as a conducting salt. When using LiBOB as the conducting salt, higher capacity retention and significantly lower dissolved iron levels were observed due to the absence of HF [8]. Additional research indicated that the use of acid scavengers in electrolytes substantially reduced Fe^{2+} dissolution [28].

3.3. Effect of Electrolyte

The electrolyte plays a critical role in lithium-ion batteries, impacting their cycling performance, power, safety, and capacity. An ideal electrolyte must exhibit exceptional electrochemical and thermodynamic stability. The commonly used electrolyte salt $LiPF_6$ in commercial LIBs is sensitive to moisture and is thermally unstable, resulting in the generation of hydrogen fluoride (HF) and phosphorus oxyfluoride (POF_3) through reactions like $LiPF_6 + H_2O/2HF + LiF + POF_3$ and accelerated thermal decomposition ($LiPF_6/LiF + PF_5$) at elevated temperatures [28]. Both PF_5 and POF_3 act as strong Lewis acids, initiating the decomposition and polymerization of cyclic carbonate solvents such as EC [45]. HF, being a strong acid, corrodes SEI layers on anodes and active cathode materials, particularly Li transition metal oxides, leading to transition metal dissolution, capacity degradation, and reduced cycle life [46–49]. While additives in the electrolyte provide partial solutions to these issues related to $LiPF_6$, the search for alternative lithium salts with high-temperature and water stability continues. LiTFSI, due to its excellent stability in heat and water, is a promising electrolyte salt for Li-ion batteries. However, its strong corrosion behavior on aluminum current collectors (Al oxidative potential around 3.7 V vs. Li/Li^+) [50] limits its application, likely linked to the mechanism of Al oxidative dissolution.

4. Modification Methods

The commercial viability of $LiFePO_4$ batteries has long been hindered by their poor high-temperature cycling stability. However, in recognition of their inherent safety and efficient performance, researchers have intensified their efforts, successfully overcoming these technical challenges. As a result, several methods have emerged to enhance their high-temperature storage capabilities. Here, we provide a concise overview of these various modification techniques.

4.1. Anode Protection

Chang et al. demonstrated that the cyclic performance of $LiFePO_4$/carbon cells could be significantly enhanced by depositing a thin layer of specific metals onto the carbon electrode [51]. Figure 6 illustrates the results of the cyclic performance tests for $LiFePO_4$/carbon cells with different metal coatings. Notably, these cells initially exhibited similar capacities around 145 mAh g^{-1} but demonstrated varying rates of capacity degradation over cycling. These can be categorized into two groups: one featuring Au and Cu coatings, which exhibited significantly reduced capacity fading, and the other with Fe, Ni, Co, or Ti coatings, showcasing faster capacity degradation compared with the pristine cell.

Scanning electron microscopy (SEM) analysis revealed a consistent correlation between the capacity fading rates and the amount of SEI deposition. Higher fading rates were associated with greater SEI material formation on the cycled carbon electrode surface. In line with Figure 6a, the Ti-coated cells exhibited the fastest capacity decay and the most abundant SEI deposition. Compared to the original battery, the iron-coated carbon electrode exhibits a more rapid capacity decay, which is consistent with the view that iron deposition on the surface of the carbon electrode can accelerate the formation of the SEI, thereby hastening capacity degradation. Cobalt and nickel coatings also react with the electrolyte to produce by-products, catalyzing the formation of SEI, leading to battery capacity degradation. Conversely, the Au-coated carbon electrode exhibited the least SEI formation, resulting in the least capacity degradation. Interestingly, the Au and Cu coatings appeared to act as "sieving layers", preventing the diffusion of metal ions into the interior of the anode layer. Consequently, by collecting Fe ions on the superficial Au and Cu layers, it became possible to reduce the overall SEI formation and mitigate capacity fading.

More surface modification strategies for anodes have also been proven to be effective in enhancing the high-temperature performance of $LiFePO_4$/carbon LIBs. Lee et al. [52] demonstrated that a carbon coating layer with a turbostratic structure, which was prepared by decomposing polyvinylchloride (PVC) on a graphite surface, protected graphite grains from electrolyte attack. They concluded that this carbon layer significantly improved the electrochemical performance and thermal stability of graphite electrodes at elevated temperatures. Another study by Park et al. [53] revealed that a thermal decomposition process involving H_3PO_4 and H_3BO_3 successfully incorporated phosphorus and boron into the surface of natural graphite, forming chemical bonds with carbon. This method results in the creation of a stable SEI film on the anode surface, reducing lithium ion consumption at high temperatures. This has proven to be an effective approach to enhance the electrochemical and thermal stabilities of natural graphite anodes in lithium-ion batteries.

In the study by Yen et al. [54], a combination of small-sized mesophase graphite (SMG) with natural graphite was investigated, with a particular focus on the impact of two different binders—polyvinylidene difluoride (PVDF) and styrene-butadiene rubber (SBR)/carboxymethyl cellulose (CMC)—on various performance aspects at elevated temperature. This included the capacity, rate capability, and cycle life of the SMG anode in an SMG/$LiFePO_4$ cell designed for high-temperature (55 °C) operation. The cycling performance (see Figure 6b) indicates that the use of an SBR/CMC binder at the anode significantly enhances the high-temperature cycle life of the entire lithium-ion battery (LIB). The surface morphologies of the SMG anodes in the 18650 cells after one and five cycles were compared, as shown in Figure 6c,d. For the anode using a PVDF binder, a relatively thick SEI layer had already formed after just one cycle, exhibiting prominent cracks and additional deposited particles on the surface (Figure 6c). In contrast, the SBR/CMC-binder anode developed a much thinner SEI layer after the first cycle, allowing the original morphology of the graphite particles to be clearly observed beneath the surface (Figure 6d). These findings indicate that the formation of the SEI layer on the SBR/CMC-binder anode was considerably slower compared with the PVDF-binder anode, which corresponded to the slower capacity fading observed in the SBR/CMC-binder cell relative to the PVDF-binder cell (Figure 6b).

In a separate investigation, Park et al. [55] presented an alternative method for anodic modification. In contrast to previous studies, their focus was on the impact of the graphite powder particle size on the thermal stability of graphite anodes. The researchers investigated the thermal stability of lithiated flake-type graphite electrodes with different particle sizes when heated in a 1.0 M $LiPF_6$ EC–DEC electrolyte. The results showed that the decomposition rate of the SEI layer accelerated with decreasing graphite particle size. Larger graphite particles, conversely, exhibited better high-temperature stability.

Subsequently, Li [56] coated $LiFePO_4$@C with SiO_2 layers using a sol–gel method. They found that the SiO_2 coating significantly improved the cycle stability of the cells by enhancing the charge transfer kinetics. This improvement was attributed to the SiO_2 layer on the particle surface, which effectively prevents direct contact between the $LiFePO_4$ particles and the electrolyte solution. As a result, the structural stability of the material is enhanced, the interfacial resistance is reduced, and the Li-ion conductivity is increased. In addition to reducing the resistance and preventing direct contact with the electrolyte, the SiO_2 coating was also believed to regulate the insertion of Li^+ into the $LiFePO_4$ structure by increasing the ordering of the outer lattice in the particles.

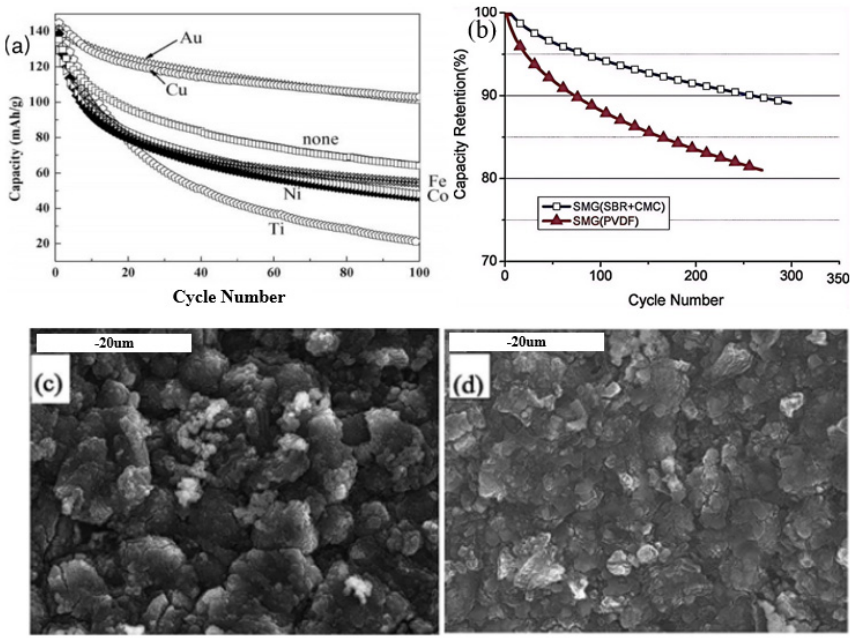

Figure 6. Cycle performance of $LiFePO_4$/MCMB cells with different metal coatings including Au, Cu, Fe, Co, Ni, and Ti on the MCMB electrode surface (**a**). All cells were cycled at 1 C charge/discharge rate at 55 °C in the voltage window of 2.5–4.0 V. The image was taken with permission [51]. Relationship between reversible capacity retention and cycle number for SMG/$LiFePO_4$ 18650 batteries containing different binders cycled at 55 °C (**b**). The image was taken with permission [54]. SEM micrographs of cycled graphitic anode containing PVDF binder after 1 cycle (**c**); SBR/CMC binder after 1 cycle (**d**). The image was taken with permission [54].

4.2. Cathode Protection

Surface coatings have been proven to be effective in mitigating issues related to high-temperature metal dissolution and cycling deterioration. In a study conducted by Yang et al. [57], a spherical porous SP-LFP/C composite was fabricated using a spray-dry (SP) method and post-sintering techniques. To enhance the high-temperature performance of the SP-LFP/C material, they employed $Li4Ti_5O_{12}$ (LTO) surface modification through the sol–gel method. The synthesis flowchart is shown in Figure 7a. The results demonstrated that the LTO-coated SP-LFP/C composite significantly mitigated the capacity fading rate at 55 °C (0.028 mA h $cycle^{-1}$) when subjected to testing at a 3 °C rate for 200 cycles. This was in stark contrast to the bare SP-LFP/C material, which exhibited a fading rate of 0.405 mA h $cycle^{-1}$. Figure 7b shows further high temperature electrochemical tests. The results showed that the SP-LFP/C cathode material with a 3% LTO coating exhibited the best cycling stability at high temperature, and less capacity degradation after 200 cycles. Interestingly, the LTO coating served a dual purpose, acting as both an ionic conductor layer to maintain high Li^+ ionic conductivity and a barrier layer to prevent Fe^{2+} dissolution. Consequently, the LTO-coated SP-LFP/C composite holds promise as a suitable candidate for lithium-ion batteries in high-power and high-temperature applications.

In addition to the aforementioned coating modification methods, elemental doping provides a viable approach [58]. Lee et al. [59] employed an anion doping method to prepare sulfur-doped $LiFePO_4$ using the traditional sol–gel method. Figure 7c illustrates the high-temperature cycling performance of sulfur-doped and unmodified $LiFePO_4$, demonstrating that the doped batteries exhibited favorable stability during high-temperature cycling. Liao et al. [60] introduced fluoride ions into $LiFePO_4$, which also led to an enhancement in the high-temperature cycle life of the battery. Furthermore, Mi et al. [61] employed a cationic doping method, uniformly introducing minor Mn into well-defined $LiFePO_4$/C

compounds. Results showed that Mn-doping contributed to an extended cycle life for the battery under high-temperature conditions.

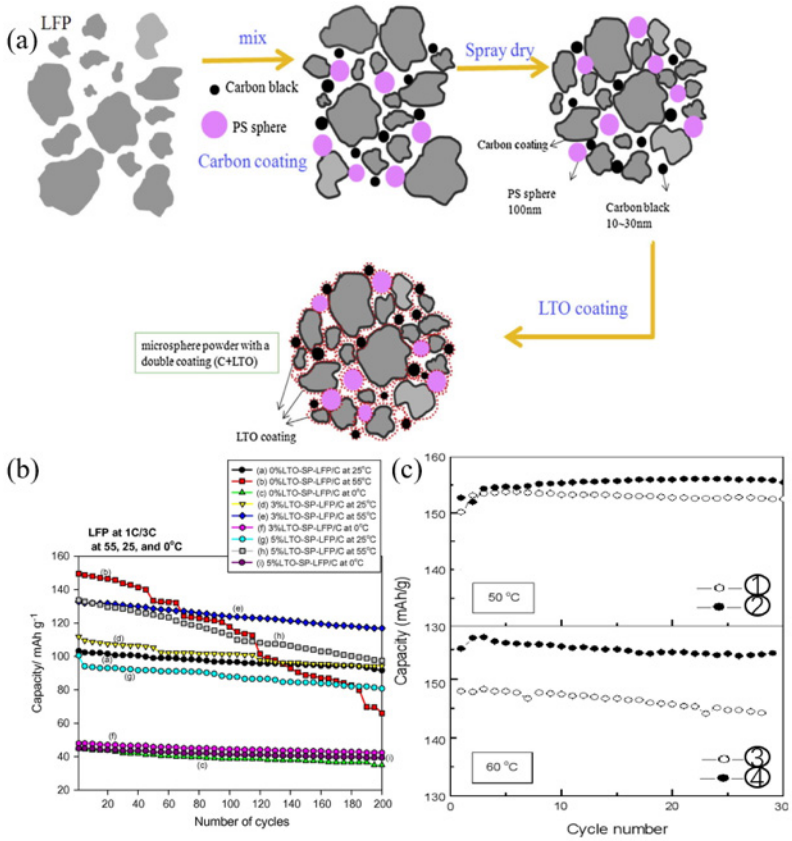

Figure 7. LTO-LFP/C synthesis flowchart (**a**). The image was taken with permission [57]. The cycling and CE performance for SS-LFP/C, SP-LFP/C and 3 and 5 wt.% LTO coated SP-LFP/C composites at 1C/3C rate at 25 and 55 °C (**b**). The image was taken with permission [57]. Cycle performances of ① $LiFePO_4$; ② $LiFePO_{3.98}S_{0.03}$ at 50 °C and ③ $LiFePO_4$; and ④ $LiFePO_{3.98}S_{0.03}$ at 60 °C (**c**). The image was taken with permission [59].

Wang [62] prepared $LiFePO_4$ material with a compacted density of 2.73 g/cm^3 by increasing the compact density of electrode laminates. The discharge energy density of the LFP/C battery (18650 cell) reached 7.0 Wh, which was 5.6–10% higher than that of the electrodes with lower compaction densities. By controlling the particle size distribution of the precursor slurry through sand grinding, they reduced the widening of the distribution range, ultimately resulting in an almost normal distribution of $LiFePO_4$/C particles. Their research demonstrates that electrodes with high compaction exhibit a lower voltage, suggesting that the highly compacted material has better wettability with the electrolyte, allowing for faster equilibrium attainment. In highly compacted battery systems, the interaction between the electrodes and the electrolyte is more stable, leading to improved performance at both high and low temperatures. Wang's study confirms these findings [62].

Yang et al. [63] synthesized a $LiFePO_4$/C-PPy composite material to enhance high-temperature stability. The resulting sample demonstrated excellent cycling stability at a 5C charge–discharge rate at 55 °C, maintaining a specific capacity retention of 140 mAh g^{-1} and preserving the discharge voltage at 3.25 V vs. Li^+/Li after 300 cycles. The notable enhancement in the electrochemical performance of the $LiFePO_4$/C-PPy electrode was attributed to improved electrical conductivity, minimal iron dissolution, and reduced electrode cracking facilitated by the PPy coating.

A well-designed surface coating layer can effectively suppress HF attack and prevent Fe dissolution. Additionally, element doping strategies can enhance the electronic conductivity of the surface-modified electrode at elevated temperatures. Therefore, combining element doping with surface decoration strategies appears to be a promising approach and warrants further investigation [64].

4.3. Electrolyte Modification

Commercial LIB electrolytes typically contain $LiPF_6$ as the conducting salt mixed with various organic carbonates [27,65–67]. However, during cycling, especially at elevated temperatures, the salt decomposition yields acidic products, such as HF, potentially leading to increased iron dissolution [27,28]. Numerous studies have explored the issue of iron dissolution from $LiFePO_4$ (LFP) into lithium-ion battery (LIB) electrolytes, attributing it to an ion exchange reaction between electrolyte-derived protons and Fe^{2+} in $LiFePO_4$ [28,40,43].

To address this concern, Amine et al. [40] improved the high-temperature performance of $LiFePO_4$/graphite cells by using a LiBOB electrolyte and $Li_4Ti_5O_{12}$ as the anode material (in which no issues related to SEI were involved as in carbon-based anodes), reducing Fe dissolution. Wu et al. [68] demonstrated that the addition of VC to the electrolyte effectively reduced Fe dissolution in $LiFePO_4$-based cells, enhancing their cycling performance at 55 °C. They evaluated two 18650-type full-cell Li-ion batteries, one containing a $LiFePO_4$ cathode and a MCMB anode with the VC additive, and the other without VC. The VC-added cell showed improved cycling performance, retaining about 80% of its initial capacity after 980 cycles at 55 °C (as shown in Figure 8a). SEM images (Figure 8b,c) revealed that the VC-containing cell displayed no deposited film on the anode's surface and preserved the granular morphology of the MCMB particles even after 100 cycles. In contrast, the non-VC cell exhibited significant Fe deposition and SEI formation on both the cathode and anode, resulting in capacity loss. ICP analysis of the cycled MCMB anodes indicated that cells containing VC had anodes with Fe contents of 50 ppm and 240 ppm after 100 and 980 cycles, respectively. In contrast, the Fe content substantially increased to 1807 ppm after just 100 cycles when VC was absent. In summary, the addition of VC additives in the electrolyte significantly enhanced the high-temperature cycling performance of the $LiFePO_4$-based Li-ion cells, suppressing Fe dissolution and SEI formation.

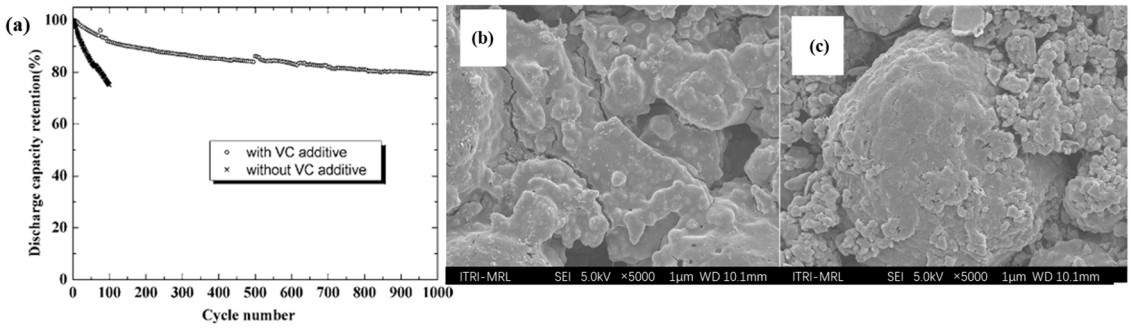

Figure 8. Comparison of the cycle life of $LiFePO_4$/graphite full cells at 55 °C (**a**); SEM micrographs of the anodes in the cells without VC (**b**) and with VC (**c**) after 100 cycles at 55 °C. The image was taken with permission [68].

Concerning the use of LiTFSI as an alternative lithium salt with high-temperature and water stability to address issues related to $LiPF_6$, a new problem emerges due to its strong corrosive behavior on aluminum current collectors (Al oxidative potential around 3.7 V vs. Li/Li^+) [50]. To inhibit Al foil corrosion at elevated temperature, a dual salt system in the electrolyte has been developed. Matsumoto et al. discovered that high LiTFSI

concentrations facilitate the formation of a protective LiF film on aluminum foil [69], while the addition of LiBOB can also help create effective passivation films on the Al foil [47,66,70]. The exact mechanisms behind this film formation have not been entirely elucidated, but it is believed that compounds from LiBOB help protect the Al foil from LiTFSI-based electrolyte corrosion. Chen et al. [71] systematically studied mixed salts of LiTFSI and LiBOB (each at >5 wt% in the electrolyte) in a $LiFePO_4$ battery system, finding that the corrosion of Al foil in LiTFSI-based electrolytes can be successfully suppressed by using LiBOB as a co-salt. This resulted in excellent high-temperature cycling stability and good room temperature rate capability, making the $LiTFSI_{0.6}$-$LiBOB_{0.4}$-based electrolyte a promising candidate for high-temperature Li-ion batteries.

However, the limited solubility and conductivity of LiBOB in carbonate solvents, especially at low temperatures and high rates, hinder its use as a sole electrolyte salt, limiting the further commercialization of lithium iron phosphate batteries. LiODFB has a structure similar to LiBOB, suggesting that its addition might protect Al foil from corrosion in LiTFSI-based electrolytes. Li et al. employed LiTFSI and LiODFB in $LiFePO_4$-based batteries and found that cells using $LiTFSI_{0.6}$-$LiODFB_{0.4}$-based electrolytes exhibited outstanding cycling stability and rate performance, surpassing cells with $LiPF_6$-based electrolytes. Adding LiODFB to LiTFSI-based electrolytes successfully suppressed Al corrosion, offering the advantage of lower cost, increased safety, competitive theoretical capacity (170 mAh g^{-1}), and higher electrical conductivity. This suggests its potential widespread use in the future [72].

Liang et al. [73] developed a room-temperature ionic liquid-based polymer electrolyte (RTIL-PE) by combining 1-butyl-1-methylpyrrolidinium bis(trifluoromethylsulfonyl)imide ([BMPy][TFSI]), LiTFSI, LiBOB, and poly(ethylene glycol) diacrylate (PEGDA). Electrochemical testing of the LFP | RTIL-PE | Li batteries showed that at 0.2 C and 50 °C, the RTIL-PE-based cell maintained an average coulombic efficiency exceeding 99.4%. The cell demonstrated a capacity retention of approximately 91.1% after 100 cycles and around 52.2% after 500 cycles, indicating excellent electrochemical stability at high temperatures. These findings suggest that RTIL-PE is a promising and safe electrolyte for next-generation electrochemical energy storage systems.

Recent studies have also highlighted the significance of drying protocols in water retention and the subsequent performance of various electrode materials. Logan et al. [74] examined the impact of water contamination and various electrolyte additives on the performance of LFP/graphite cells. Consistent with earlier findings, the presence of electrolyte additives, such as VC [68], mitigated capacity degradation at high temperatures, thereby enhancing the cycling stability of the batteries. In contrast, cells with no electrolyte additives (control electrolyte) exhibited poor performance, which could be significantly improved by vacuum drying the cells at higher temperatures to remove excess water.

4.4. Binder, Separator and Current Collectors Modification

The performance of lithium-ion batteries is primarily determined by the properties of the electrode active materials and electrolytes, as previously discussed. However, binders also play a crucial role in influencing the electrochemical performance of these batteries. They affect electronic and ionic conductivity, connect electrode assemblies, and maintain electrode cohesion over time [75,76].

Polyvinylidene fluoride (PVDF) is one of the most commonly used polymer binders in lithium-ion batteries. However, PVDF is expensive, difficult to recycle, and requires the use of hazardous solvents such as N-methyl-2-pyrrolidone (NMP), which is toxic and environmentally damaging [77]. Furthermore, its high-temperature stability is limited. To address these issues, water-soluble alternatives are being explored to enhance the electrochemical performance of lithium-ion batteries. Water-based binders also offer an

environmentally friendly manufacturing approach [78]. In one study by Ding et al. [79], a new three-component polymer gel binder (PGB) was developed, consisting of chitosan, an ionic liquid (1-butyl-1-methylpyrrolidinium dicyanamide (PYR14 DCA)), and LiTFSI for use in $LiFePO_4$ electrodes. The addition of PYR14 DCA increases the availability of free amino and hydroxy groups by dissociating chitosan chains, enhancing the binding of each electrode component to the current collector. Their research demonstrated that LFP/PGB exhibited stable cycling performance at 60 °C, with a capacity retention of approximately 70% after 100 cycles at a high rate of 10 C (corresponds to a current that enables full charge or discharge in 6 minutes). Additionally, Ding et al. [80] prepared thick electrodes (4.5 mg cm^{-2} mass loading) using a simple coating process. Their study showed that LFP/PGB electrodes exhibited significantly better rate capabilities compared with LFP/PVDF electrodes across all C-rates. At a particularly high current density of 30 C, LFP/PGB still maintained a steady capacity of at least 123 mAh g^{-1}, while LFP/PVDF electrodes showed a near-zero capacity. This enhanced performance was attributed to the improved electronic conductivity provided by carbon black particles along the chitosan polymer chains and the increased lithium-ion transfer ability from the addition of LiTFSI and the ionic liquid. In summary, the PGB binder's unique composition overcomes the limitations of PVDF, improving the electrochemical performance, particularly at elevated temperatures, and thus enhancing the high-temperature cycling stability of $LiFePO_4$ batteries.

Separators are also vital components of lithium-ion batteries, serving not only as porous channels for ionic transport but also as barriers preventing physical contact between the anode and cathode [81]. One of the key reasons for poor high-temperature cycling performance in $LiFePO_4$ batteries is the dissolution of iron at elevated temperatures, leading to its deposition on the anode and significant capacity degradation. Therefore, designing diaphragms with excellent mechanical properties and high thermal stability is essential to improve the high-temperature cycling performance of lithium iron phosphate batteries.

Several factors must be considered when designing high-performance diaphragms. They must be chemically inert under both reduction and oxidation conditions in organic electrolyte solutions. Additionally, diaphragms should have high porosity to allow for ion flow, but sufficient tortuosity to prevent the growth of lithium dendrites. They must also be absorbent to maintain electrolyte wettability, mechanically robust, and thermally stable over a wide range of temperatures. Moreover, diaphragms should exhibit good flame retardancy and high ionic conductivity, with an ionic transference number approaching unity. Currently, commercial separators, such as Celgard separators, are typically made from porous polyolefin films like polypropylene (PP), polyethylene (PE), or a mixture of these materials [82].

In recent years, several innovative strategies have been employed to design and prepare lithium-ion battery separators, with many new separators emerging beyond conventional polyolefin-based designs. One strategy involves coating inorganic particles on the surface of polyolefin-based separators to enhance their properties. For example, a polyacrylonitrile separator with increased porosity and improved electrolyte wettability can be fabricated using an electrospinning method [83], while Al_2O_3-modified polyolefin membranes offer better electrolyte wettability and thermal stability [84]. Another approach is to develop full-inorganic separators to improve the thermal stability of the battery. These can include SiO_2 particles that self-assemble into hollow mesoporous structures [85] or nonwoven ZrO_2 ceramic membranes with robust nanofiber microstructures [86]. Despite these advances, challenges remain in developing separators that balance high porosity, excellent electrolyte wettability, thermal stability, and mechanical strength [87].

In a recent study, a polyacrylonitrile/boric acid/melamine/delaminated BN nanosheet electrospun fiber membrane (PB_3N_1BN) was fabricated, which exhibited excellent mechanical properties, high thermal stability, superior flame-retardant performance, and good electrolyte wettability [82]. The electrochemical behavior of this PB_3N_1BN membrane was evaluated in high-temperature conditions, with devices assembled using $LiFePO_4/PB_3N_1BN/Li$ and $LiFePO_4/PP/Li$ tested at 80 °C and 100 °C. The results showed that the $LiFePO_4/PB_3N_1BN/Li$ device maintained a high capacity of 152 mAh g^{-1} at 1.0 C without significant capacity decay after 60 cycles at 80 °C. In contrast, the $LiFePO_4/PP/Li$ device exhibited a notable capacity reduction, with only 137 mAh g^{-1} remaining. These findings indicate that the $LiFePO_4/PB_3N_1BN/Li$ device demonstrates excellent electrochemical stability at high temperatures, and the PB_3N_1BN electrospun fiber membrane shows promising potential as a separator for lithium-ion batteries.

In addition to this, the modification of the collector can also enhance the stability of LFP cells and mitigate the dissolution of transition metals at high temperatures. The most common method of collector modification is carbon coating.

Graphite carbon has high thermal stability, excellent electrical conductivity, industrial reliability, low cost, and most importantly, non-toxicity, which make it a preferred choice for collector carbon-coating materials in a variety of applications [88,89]. The category of graphitic carbons includes a wide range of materials such as carbon nanotubes (CNTs), graphene, graphene oxide (GO), reduced GO (rGO), graphdiyne (GDY), and so forth. It improves the electronic conductivity of the collector, reduces the interfacial resistance between the electrode material and the collector, and establishes a stable interface that ultimately improves the overall performance and life cycle of the battery. In addition, the carbon layer acts as a protective barrier to prevent aluminum from corroding or reacting with the electrolyte, especially at higher potentials. While the addition of a graphite-carbon coating adds an extra step to the manufacturing process, which may increase costs, the improvement in battery life and performance often outweighs this drawback. Cost-effectiveness also depends on the scale of production; for large-scale production, economies of scale can make the coating process more affordable. However, for small-scale or customized applications, the additional costs may be more significant. Introducing graphitic carbon coatings into aluminum current collectors can complicate the manufacturing process. The coating must be uniform, adhere well to the aluminum surface, and maintain its integrity during battery cycling [88].

4.5. State-of-Charge (SOC) Control

Early studies suggest that maintaining $LiFePO_4$-based LIBs within a medium state-of-charge (SOC) range enhances their stability compared with high or low SOC cycling (Figure 9a) [90]. Electrochemical tests, such as GITT and EIS analyses, reveal higher impedance polarization in $LiFePO_4$/carbon LIBs cycled at high or low SOC. This results from pronounced side reactions between the electrolytes and electrodes and visible structural changes in both the $LiFePO_4$ and anode materials during very high or very low SOC conditions. Precise SOC control mitigates degradation, bolsters $LiFePO_4$/carbon LIB cycling stability, and aids in accurate performance degradation prediction models [91]. Nevertheless, Sauer et al. found that cycling degradation at 1 C between 45% and 55% SOC exceeded that between 50% and 100% depth-of-discharge (DOD) [92]. Furthermore, cycling at 4.0 C displayed a lower degradation rate than at lower charge/discharge rates (Figure 9b), warranting further investigation. Molaeimanesh et al. [93] investigated the cycling performance of lithium iron phosphate (LFP) batteries under different state-of-charge (SOC) conditions (30%, 50%, and 100%) at 55 °C. The results revealed that capacity degradation was minimal at 50% SOC, while it was most severe at 100% SOC. These findings

suggest that maintaining the battery around 50% SOC is an effective strategy to minimize capacity loss and enhance battery longevity.

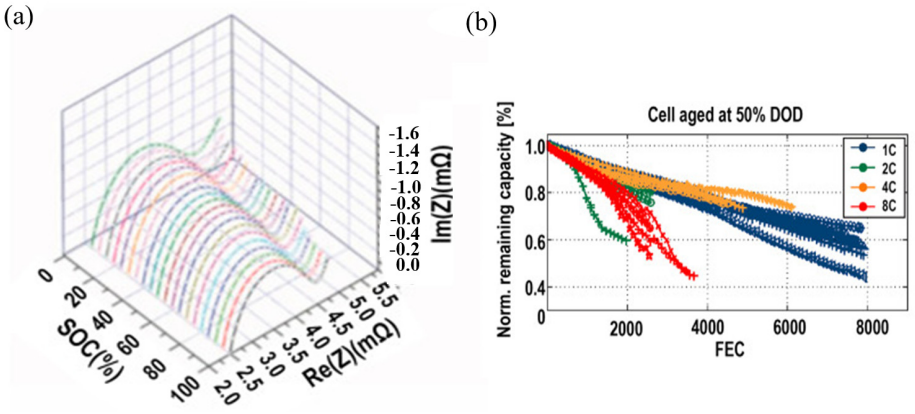

Figure 9. EIS at different SOC values when charging, with 10 min rest time at 25 °C (**a**). The image was taken with permission [90]. Trend in the relative capacity of the cycle degradation tests at 50% DOD and C-rates of 1.0, 2.0, 4.0, and 8.0 C at 40 °C (**b**). The images were taken with permission [92].

4.6. Thermal Runaway Detection

In addition to the aforementioned improvement methods, thermal runaway (TR) detection technology for lithium iron phosphate batteries presents a valuable approach to enhance safety.

Jia et al. [94] outlined the thermal runaway chain reaction of LFP batteries in four distinct stages, as illustrated in Figure 10a. In stage I, the LFP battery is subjected to external abuse conditions. This leads to self-heating, marking the transition to stage II. Once the SEI layer decomposes, the lithiated graphite anode loses its protective layer, allowing it to react with the electrolyte, which generates heat and gas. As the electrolyte evaporates and gas is produced under high temperatures, the internal pressure of the battery gradually rises. When this pressure reaches the threshold value of the safety valve's opening pressure, the valve opens. In stage III, the opening of the safety valve releases large amounts of gases, liquids, and solid particles from inside the battery. This can lead to gas venting and potential flame behavior, resulting in thermal runaway in stage IV. Therefore, effective monitoring and early warning systems are crucial for managing battery safety.

In the effective management of battery system safety, a well-designed temperature monitoring strategy is essential. This strategy should include tracking both the battery's temperature and its rate of temperature rise, with particular attention to sudden changes in the temperature rise rate, which can serve as an early warning for potential issues [95,96]. Zhou et al. [97] highlighted that research in China has focused on developing early warning technologies for battery thermal runaway given the multiple factors that can trigger such events. These technologies utilize various monitoring systems tailored to specific risks. For example, thermal runaway due to overheating can be detected through single-unit temperature or temperature rise monitoring systems. Overcharging, over-discharging, and internal short-circuit initiation within the battery can be monitored via a single-voltage monitoring system. Jia et al. [94] analyzed the warning signals of eight key parameters of the battery system and summarized their response order as follows: temperature signal → infrared imaging → gas pressure and external stress → EIS signal → voltage signal → sound signal → ejection image recognition → gas signal. The sequence and advantages of these response signals are outlined in Figure 10b. The first five warning signals occur before safety venting, which is generally considered to be an early warning. Among these, the temperature and pressure signals are the earliest to respond due to the heat and gas generation characteristics of LFP batteries during the early stages of thermal

runaway (TR). However, these warning methods require monitoring individual batteries or modules, which can be costly and complex to implement. In contrast, sound, smoke, and gas signals in the battery energy storage container (BESC) are more cost-effective and easier to manage. These signals can also provide warnings after safety venting, which is widely used in BESCs. Li et al. [98] proposed a multidimensional parameter detection strategy to identify TR in LFP battery modules, enabling earlier and more accurate warnings using parameters such as practical expansion force, temperature, and voltage [99]. Based on this, we recommend a composite warning strategy combining expansion force and characteristic gas detection for large-scale battery energy storage systems (BESSs), focusing on the battery module and BESC two-level warning to ensure efficient and accurate early warnings. Additionally, the monitoring of gas concentration, insulation degradation, ultrasonic detection, and fiber-optic pressure detection systems can help identify risks such as battery breakage, leakage, lithium dendrite growth, or the intensification of internal side reactions.

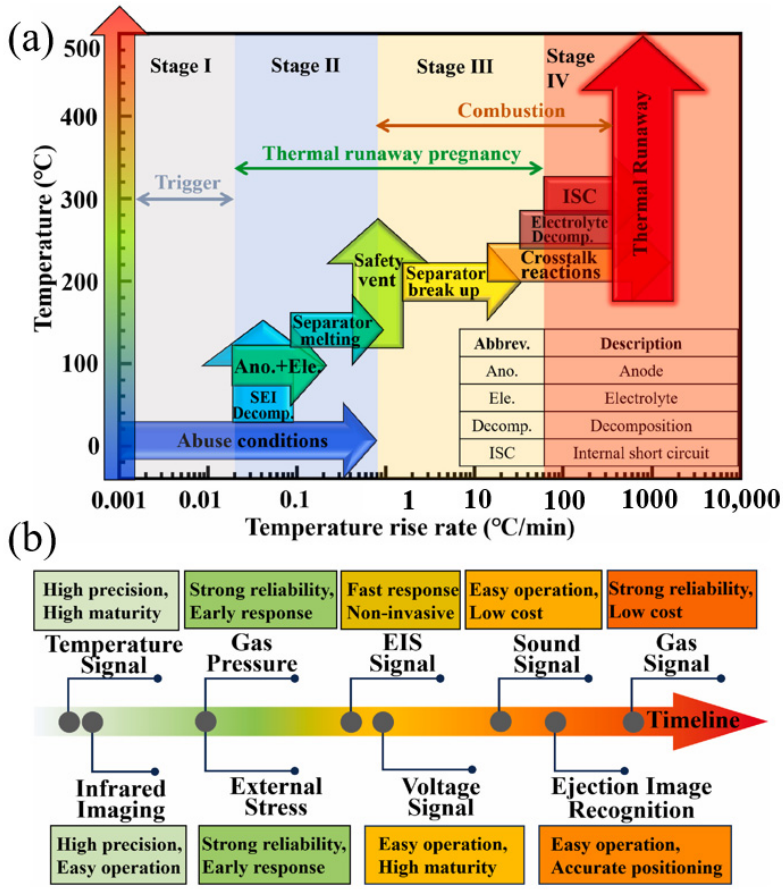

Figure 10. Chain reactions of LFP batteries during TR (**a**). The images were taken with permission [94]. The sequence and advantages of warning signal response (**b**).The images were taken with permission [94].

To further ensure the battery's safety, cooling systems, such as air cooling or liquid cooling can be employed to maintain the internal temperature within a safe range. This helps prevent overheating and ensures that the battery operates smoothly. Zhou et al. [97] also emphasized that safety protection measures for $LiFePO_4$ batteries should begin with a thorough inspection of the battery body and continue throughout its entire life cycle. This proactive approach can significantly reduce the risk of safety incidents during operation, thereby safeguarding the overall safety of energy storage power stations.

4.7. Simulation and Forecasting

Density functional theory (DFT), which was applied earlier in the field of electrochemical energy storage, is a quantum mechanical method used to calculate the electronic structure and properties of materials, and can simulate the atomic structure, ion diffusion rate, and phase transition temperature of materials [100,101]. Machine learning (ML) has been widely used in the battery field in the last few years, and it can be used to process large amounts of data, predict material properties, optimize the experimental parameters, and so on [101–103]. ML and DFT play a key role in improving the high temperature performance of LFP batteries, and the combination of the two significantly accelerates material design optimization and performance prediction.

DFT reveals atomic-scale mechanisms through quantum mechanical calculations to provide theoretical guidance for high-temperature property optimization such as calculating the migration energy barriers of Li^+ at different crystalline surfaces (e.g., (010) channel) to guide doping (e.g., Mg^{2+}, Ti^{4+}) to broaden the diffusion channels and predict the inhibitory effect of doping elements (e.g., Co, Ni) on the LFP lattice distortion to reduce the volume expansion at high temperatures. ML dramatically shortens experimental cycles through high-throughput screening and performance prediction such as modeling the correlation between elemental doping (e.g., cation substitution, anion doping) and high-temperature cycling performance, and predicting the optimal doping ratio [104]. The synergistic effect of DFT and ML can perform a multi-scale modeling framework and accelerate research and development (R&D) through active learning. The former can generate microscopic data (e.g., migration barriers, surface energy) by DFT as ML input to build cross-scale performance prediction models such as combining interfacial binding energies computed by DFT with ML modeling to predict the inhibitory effect of carbon cladding thickness on high-temperature Fe dissolution. The latter is formed by the ML recommendation of potential candidate materials → DFT verification of key properties → experimental synthesis and validation, forming a closed-loop iteration [101].

In conclusion, machine learning through data-driven efficient screening and density flood theory through in-depth analysis of microscopic mechanisms synergistically provide a full chain solution from atomic design to system integration for the optimization of the high-temperature performance of LFP batteries. With the upgrading of computing resources and algorithmic innovation in the future, this cross-cutting field is expected to promote the rapid realization of the next-generation high-security and long-life energy storage devices.

5. Conclusions and Future Outlooks

In this comprehensive review, we systematically summarized the challenges and strategies associated with the high-temperature stability of $LiFePO_4$/carbon lithium-ion batteries. While $LiFePO_4$ offers advantages such as cost-effectiveness, safety, and thermal stability, its performance at elevated temperatures is hindered by Fe^{2+} dissolution, electrolyte decomposition, and SEI layer growth. Various modification strategies have been explored including anode and cathode surface modifications, electrolyte optimization, binder and separator innovations, state-of-charge (SOC) control, thermal runaway detection and prevention as well as computational and machine learning approaches.

While significant progress has been made in improving the high-temperature stability of $LiFePO_4$/carbon batteries, several areas warrant further investigation:

(1) Advanced coating materials: Future research should focus on developing novel coating materials with enhanced thermal and electrochemical stability. Exploring nanomaterials and hybrid coatings could further mitigate Fe dissolution and SEI growth.

(2) Electrolyte additives and salts: The development of new electrolyte additives and salts with improved thermal stability and reduced reactivity with electrode materials is crucial. Research into ionic liquids and solid-state electrolytes could offer promising alternatives.
(3) Binder and separator optimization: Continued innovation in binder and separator materials is needed to enhance their thermal stability, mechanical strength, and ionic conductivity. The integration of flame-retardant properties into separators could further improve battery safety.
(4) SOC management strategies: Further studies are required to optimize SOC control strategies, particularly for large-scale battery systems. Developing adaptive SOC management algorithms could enhance battery longevity and performance under varying thermal conditions.
(5) Thermal management systems: Advanced thermal management systems, including phase-change materials and active cooling technologies, should be explored to maintain the optimal operating temperatures and prevent thermal runaway.
(6) Machine learning and DFT integration: The integration of machine learning and DFT for high-throughput screening and material design holds great potential. Future research should focus on developing multi-scale models that can predict battery performance under high-temperature conditions and guide the synthesis of new materials.
(7) Real-world validation: While laboratory-scale studies have provided valuable insights, real-world validation of these strategies in commercial battery systems is essential. Long-term cycling tests under realistic operating conditions will help identify practical challenges and refine modification strategies.
(8) Sustainability and recycling: As the demand for $LiFePO_4$ batteries grows, research into sustainable production methods and recycling technologies will be critical. Developing eco-friendly manufacturing processes and efficient recycling techniques will ensure the long-term viability of $LiFePO_4$-based energy storage systems.

In conclusion, the high-temperature stability of $LiFePO_4$/carbon batteries remains a critical area of research, with significant potential for improvement through material modifications, advanced electrolytes, and innovative thermal management strategies. By addressing these challenges, $LiFePO_4$ batteries can continue to play a pivotal role in the transition to sustainable energy storage solutions.

Author Contributions: Conceptualization, R.X.; Writing—original draft preparation, G.J., W.Z. and J.Z.; Writing—review and editing, W.L. and M.C.; Supervision, R.X. All authors have read and agreed to the published version of the manuscript.

Funding: This research was funded by the National Natural Science Foundation of China (grant number 52102204) and the Fundamental Research Funds for the Central Universities (grant number FRF-TP-24-001A).

Institutional Review Board Statement: Not applicable.

Data Availability Statement: No new data were created or analyzed in this study.

Acknowledgments: Mingyang Chen would like to thank the Startup funding from the University of Science and Technology Beijing.

Conflicts of Interest: The authors declare no conflicts of interest. The funders had no role in the design of the study; in the collection, analyses, or interpretation of data; in the writing of the manuscript; or in the decision to publish the results.

References

1. Padhi, A.K.; Nanjundaswamy, K.S.; Goodenough, J.B. Phospho-olivines as Positive-Electrode Materials for Rechargeable Lithium Batteries. *J. Electrochem. Soc.* **1997**, *144*, 1188–1194. [CrossRef]
2. Zheng, Y.J.; Ouyang, M.G.; Lu, L.G.; Li, J.Q.; Han, X.B.; Xu, L.F.; Ma, H.B.; Dollmeyer, T.A.; Freyermuth, V. Cell state-of-charge inconsistency estimation for $LiFePO_4$ battery pack in hybrid electric vehicles using mean-difference model. *Appl. Energy* **2013**, *111*, 571–580. [CrossRef]
3. Choi, D.W.; Wang, D.H.; Viswanathan, V.V.; Bae, I.T.; Wang, W.; Nie, Z.M.; Zhang, J.G.; Graff, G.L.; Liu, J.; Yang, Z.G.; et al. Li-ion batteries from $LiFePO_4$ cathode and anatase/graphene composite anode for stationary energy storage. *Electrochem. Commun.* **2010**, *12*, 378–381. [CrossRef]
4. Damen, L.; Hassoun, J.; Mastragostino, M.; Scrosati, B. Solid-state, rechargeable $Li/LiFePO_4$ polymer battery for electric vehicle application. *J. Power Sources* **2010**, *195*, 6902–6904. [CrossRef]
5. Gatta, F.M.; Geri, A.; Lamedica, R.; Lauria, S.; Maccioni, M.; Palone, F.; Rebolini, M.; Ruvio, A. Application of a $LiFePO_4$ Battery Energy Storage System to Primary Frequency Control: Simulations and Experimental Results. *Energies* **2016**, *9*, 887. [CrossRef]
6. Huang, Y.H.; Park, K.S.; Goodenough, J.B. Improving lithium batteries by tethering carbon-coated $LiFePO_4$ to polypyrrole. *J. Electrochem. Soc.* **2006**, *153*, A2282–A2286. [CrossRef]
7. Lian, B.; Sims, A.; Yu, D.M.; Wang, C.; Dunn, R.W. Optimizing $LiFePO_4$ Battery Energy Storage Systems for Frequency Response in the UK System. *IEEE Trans. Sustain. Energy* **2017**, *8*, 385–394. [CrossRef]
8. Zhang, W.J. Structure and performance of $LiFePO_4$ cathode materials: A review. *J. Power Sources* **2011**, *196*, 2962–2970. [CrossRef]
9. Carrilero, I.; González, M.; Anseán, D.; Viera, J.C.; Chacón, J.; Pereirinha, P.G. (Eds.) Redesigning European Public Transport: Impact of New Battery Technologies in the Design of Electric Bus Fleets. In Proceedings of the 13th Conference on Transport Engineering (CIT), Gijon, Spain, 6–8 June 2018.
10. Csernáth, G.; Turos, L. (Eds.) Embeddable, smart, DC operated UPS for small and mid sized battery backup applications. In Proceedings of the 13th International Conference on Optimization of Electridcal and Electronic Equipment, Brasov, Romania, 24–26 May 2012. (In Romania).
11. Kontorinis, V.; Zhang, L.E.; Aksanli, B.; Sampson, J.; Homayoun, H.; Pettis, E.; Tullsen, D.M.; Rosing, T.S.; IEEE (Eds.) Managing Distributed UPS Energy for Effective Power Capping in Data Centers. In Proceedings of the 39th Annual International Symposium on Computer Architecture (ISCA), Portland, OR, USA, 9–13 June 2012.
12. Stan, A.I.; Swierczynski, M.; Stroe, D.I.; Teodorescu, R.; Andreasen, S.J.; Moth, K.; IEEE (Eds.) A Comparative Study of Lithium Ion to Lead Acid Batteries for use in UPS Applications. In Proceedings of the 36th IEEE International Conference on Telecommunications Energy Conference (INTELEC), Vancouver, BC, Canada, 28 September–2 October 2014.
13. Berckmans, G.; Messagie, M.; Smekens, J.; Omar, N.; Vanhaverbeke, L.; Van Mierlo, J. Cost Projection of State of the Art Lithium-Ion Batteries for Electric Vehicles Up to 2030. *Energies* **2017**, *10*, 1314. [CrossRef]
14. Scrosati, B.; Garche, J. Lithium batteries: Status, prospects and future. *J. Power Sources* **2010**, *195*, 2419–2430. [CrossRef]
15. Jung, S.; Kang, D. Multi-dimensional modeling of large-scale lithium-ion batteries. *J. Power Sources* **2014**, *248*, 498–509. [CrossRef]
16. Li, Z.; Zhang, D.; Yang, F. Developments of lithium-ion batteries and challenges of $LiFePO_4$ as one promising cathode material. *J. Mater. Sci.* **2009**, *44*, 2435–2443. [CrossRef]
17. Hu, J.; Huang, W.; Yang, L.; Pan, F. Structure and performance of the $LiFePO_4$ cathode material: From the bulk to the surface. *Nanoscale* **2020**, *12*, 15036–15044. [CrossRef] [PubMed]
18. Zhang, Y.; Huo, Q.Y.; Du, P.P.; Wang, L.Z.; Zhang, A.Q.; Song, Y.H.; Lv, Y.; Li, G.Y. Advances in new cathode material $LiFePO_4$ for lithium-ion batteries. *Synth. Met.* **2012**, *162*, 1315–1326. [CrossRef]
19. Zhou, W.; Sit, P.H.L. First-Principles Understanding of the Staging Properties of the Graphite Intercalation Compounds towards Dual-Ion Battery Applications. *ACS Omega* **2020**, *5*, 18289–18300. [CrossRef] [PubMed]
20. Cheng, H.; Shapter, J.G.; Li, Y.; Gao, G. Recent progress of advanced anode materials of lithium-ion batteries. *J. Energy Chem.* **2021**, *57*, 451–468. [CrossRef]
21. Cheng, Y.L.; Li, T.H.; Li, F.J.; Zhuang, Q.; Jing, D.Q. Preparation of Mesocarbon Microbeads and Subsequent Heating Treatment. *Int. J. Chem. React. Eng.* **2009**, *7*, 18. [CrossRef]
22. Li, H.; Zheng, C.; Qi, J.; Wang, H. Crude Mesocarbon Microbeads as an Economical and Efficient Electrode Material for Safe Symmetrical-Carbon Cells. *ACS Appl. Energy Mater.* **2023**, *6*, 4327–4333. [CrossRef]
23. Guo, A.J.; Wang, F.; Jiao, S.H.; Ibrahim, U.K.; Liu, D.; Liu, H.; Chen, K.; Wang, Z.X. Preparation of mesocarbon microbeads as anode material for lithium-ion battery by thermal polymerization of a distillate fraction from an FCC slurry oil after hydrofining with suspended catalyst. *Fuel Process. Technol.* **2020**, *276*, 118037. [CrossRef]
24. Hu, X.B.; Zhao, B.Y.; Hu, K.A. Thermal behaviors of mesocarbon microbeads and physical properties of carbon plates. *J. Mater. Sci.* **2004**, *39*, 1735–1741. [CrossRef]
25. Verrelli, R.; Hassoun, J. High-Capacity NiO-(Mesocarbon Microbeads) Conversion Anode for Lithium-Ion Battery. *ChemElectroChem* **2015**, *2*, 988–994. [CrossRef]

26. Zhang, D.K.; Zhang, L.Z.; Yu, Y.; Zhang, L.; Xu, Z.M.; Sun, X.W.; Zhao, S.Q. Mesocarbon Microbead Production from Fluid Catalytic Cracking Slurry Oil: Improving Performance through Supercritical Fluid Extraction. *Energy Fuels* **2018**, *32*, 12477–12485. [CrossRef]
27. Campion, C.L.; Li, W.T.; Lucht, B.L. Thermal decomposition of $LiPF_6$-based electrolytes for lithium-ion batteries. *J. Electrochem. Soc.* **2005**, *152*, A2327–A2334. [CrossRef]
28. Koltypin, M.; Aurbach, D.; Nazar, L.; Ellis, B. On the stability of $LiFePO_4$ olivine cathodes under various conditions (electrolyte solutions, temperatures). *Electrochem. Solid State Lett.* **2007**, *10*, A40–A44. [CrossRef]
29. Xu, K.; Zhang, S.S.; Lee, U.; Allen, J.L.; Jow, T.R. LiBOB: Is it an alternative salt for lithium ion chemistry? *J. Power Sources* **2005**, *146*, 79–85. [CrossRef]
30. Li, J.; Xie, K.; Lai, Y.; Zhang, Z.a.; Li, F.; Hao, X.; Chen, X.; Liu, Y. Lithium oxalyldifluoroborate/carbonate electrolytes for $LiFePO_4$/artificial graphite lithium-ion cells. *J. Power Sources* **2010**, *195*, 5344–5350. [CrossRef]
31. Li, D.J.; Danilov, D.L.; Xie, J.; Raijmakers, L.; Gao, L.; Yang, Y.; Notten, P.H.L. Degradation Mechanisms of C_6/$LiFePO_4$ Batteries: Experimental Analyses of Calendar Aging. *Electrochim. Acta* **2016**, *190*, 1124–1133. [CrossRef]
32. Sun, S.; Guan, T.; Shen, B.; Leng, K.Y.; Gao, Y.Z.; Cheng, X.Q.; Yin, G.P. Changes of Degradation Mechanisms of $LiFePO_4$/Graphite Batteries Cycled at Different Ambient Temperatures. *Electrochim. Acta* **2017**, *237*, 248–258. [CrossRef]
33. Kabir, M.M.; Demirocak, D.E. Degradation mechanisms in Li-ion batteries: A state-of-the-art review. *Int. J. Energy Res.* **2017**, *41*, 1963–1986. [CrossRef]
34. Guo, Z.J.; Chen, Z.L. High-temperature capacity fading mechanism for $LiFePO_4$/graphite soft-packed cell without Fe dissolution. *J. Electroanal. Chem.* **2015**, *754*, 148–153. [CrossRef]
35. Kassem, M.; Delacourt, C. Postmortem analysis of calendar-aged graphite/$LiFePO_4$ cells. *J. Power Sources* **2013**, *235*, 159–171. [CrossRef]
36. Lewerenz, M.; Warnecke, A.; Sauer, D.U. Post-mortem analysis on $LiFePO_4$ | Graphite cells describing the evolution & composition of covering layer on anode and their impact on cell performance. *J. Power Sources* **2017**, *369*, 122–132.
37. Liu, P.; Wang, J.; Hicks-Garner, J.; Sherman, E.; Soukiazian, S.; Verbrugge, M.; Tataria, H.; Musser, J.; Finamore, P. Aging Mechanisms of $LiFePO_4$ Batteries Deduced by Electrochemical and Structural Analyses. *J. Electrochem. Soc.* **2010**, *157*, A499–A507. [CrossRef]
38. Lai, Y.Q.; Cao, Z.; Song, H.S.; Zhang, Z.A.; Chen, X.; Lu, H.; Jia, M.; Li, J. Influence of Fe (II) Species in Electrolyte on Performance of Graphite Anode for Lithium-Ion Batteries. *J. Electrochem. Soc.* **2012**, *159*, A1961–A1966. [CrossRef]
39. Iltchev, N.; Chen, Y.K.; Okada, S.; Yamaki, J. $LiFePO_4$ storage at room and elevated temperatures. *J. Power Sources* **2003**, *119*, 749–754. [CrossRef]
40. Amine, K.; Liu, J.; Belharouak, I. High-temperature storage and cycling of C-$LiFePO_4$/graphite Li-ion cells. *Electrochem. Commun.* **2005**, *7*, 669–673. [CrossRef]
41. Komaba, S.; Kumagai, N.; Kataoka, Y. Influence of manganese(II), cobalt(II), and nickel(II) additives in electrolyte on performance of graphite anode for lithium-ion batteries. *Electrochim. Acta* **2002**, *47*, 1229–1239. [CrossRef]
42. Li, D.; Danilov, D.L.; Zwikirsch, B.; Fichtner, M.; Yang, Y.; Eichel, R.-A.; Notten, P.H.L. Modeling the degradation mechanisms of C_6/$LiFePO_4$ batteries. *J. Power Sources* **2018**, *375*, 106–117. [CrossRef]
43. Striebel, K.; Shim, J.; Sierra, A.; Yang, H.; Song, X.Y.; Kostecki, R.; McCarthy, K. The development of low cost $LiFePO_4$-based high power lithium-ion batteries. *J. Power Sources* **2005**, *146*, 33–38. [CrossRef]
44. Zaghib, K.; Ravet, N.; Gauthier, M.; Gendron, F.; Mauger, A.; Goodenough, J.B.; Julien, C.M. Optimized electrochemical performance of $LiFePO_4$ at 60 °C with purity controlled by SQUID magnetometry. *J. Power Sources* **2006**, *163*, 560–566. [CrossRef]
45. Sloop, S.E.; Pugh, J.K.; Wang, S.; Kerr, J.B.; Kinoshita, K. Chemical reactivity of PF_5 and $LiPF_6$ in ethylene carbonate/dimethyl carbonate solutions. *Electrochem. Solid State Lett.* **2001**, *4*, A42–A44. [CrossRef]
46. Arora, P.; White, R.E.; Doyle, M. Capacity fade mechanisms and side reactions in lithium-ion batteries. *J. Electrochem. Soc.* **1998**, *145*, 3647–3667. [CrossRef]
47. Shieh, D.T.; Hsieh, P.H.; Yang, M.H. Effect of mixed LiBOB and $LiPF_6$ salts on electrochemical and thermal properties in $LiMn_2O_4$ batteries. *J. Power Sources* **2007**, *174*, 663–667. [CrossRef]
48. Sinha, N.N.; Burns, J.C.; Sanderson, R.J.; Dahn, J. Comparative Studies of Hardware Corrosion at High Potentials in Coin-Type Cells with Non Aqueous Electrolytes. *J. Electrochem. Soc.* **2011**, *158*, A1400–A1403. [CrossRef]
49. Yang, H.; Zhuang, G.V.; Ross, P.N. Thermal stability of $LiPF_6$ salt and Li-ion battery electrolytes containing $LiPF_6$. *J. Power Sources* **2006**, *161*, 573–579. [CrossRef]
50. Péter, L.; Arai, J. Anodic dissolution of aluminium in organic electrolytes containing perfluoroalkylsulfonyl imides. *J. Appl. Electrochem.* **1999**, *29*, 1053–1061. [CrossRef]
51. Chang, H.H.; Wu, H.C.; Wu, N.L. Enhanced high-temperature cycle performance of $LiFePO_4$/carbon batteries by an ion-sieving metal coating on negative electrode. *Electrochem. Commun.* **2008**, *10*, 1823–1826. [CrossRef]

52. Lee, H.Y.; Baek, J.K.; Lee, S.M.; Park, H.K.; Lee, K.Y.; Kim, M.H. Effect of carbon coating on elevated temperature performance of graphite as lithium-ion battery anode material. *J. Power Sources* **2004**, *128*, 61–66. [CrossRef]
53. Park, M.S.; Lee, J.; Lee, J.W.; Kim, K.J.; Jo, Y.N.; Woo, S.G.; Kim, Y.J. Tuning the surface chemistry of natural graphite anode by H_3PO_4 and H_3BO_3 treatments for improving electrochemical and thermal properties. *Carbon* **2013**, *62*, 278–287. [CrossRef]
54. Yen, J.P.; Lee, C.M.; Wu, T.L.; Wu, H.C.; Su, C.Y.; Wu, N.L.; Hong, J.L. Enhanced High-Temperature Cycle-Life of Mesophase Graphite Anode with Styrene-Butadiene Rubber/Carboxymethyl Cellulose Binder. *Ecs Electrochem. Lett.* **2012**, *1*, A80–A82. [CrossRef]
55. Park, Y.S.; Lee, S.M. Effects of particle size on the thermal stability of lithiated graphite anode. *Electrochim. Acta* **2009**, *54*, 3339–3343. [CrossRef]
56. Li, Y.-D.; Zhao, S.-X.; Nan, C.-W.; Li, B.-H. Electrochemical performance of SiO_2-coated $LiFePO_4$ cathode materials for lithium ion battery. *J. Alloys Compd.* **2011**, *509*, 957–960. [CrossRef]
57. Yang, C.C.; Jang, J.H.; Jiang, J.R. Study of electrochemical performances of lithium titanium oxide-coated $LiFePO_4$/C cathode composite at low and high temperatures. *Appl. Energy* **2016**, *162*, 1419–1427. [CrossRef]
58. Jiao, L.X.; Li, Z.Q.; Zhu, Y.Z.; Wei, Z.; Liang, Y.; Wang, X.L.; Cui, Y.; Zhang, Z.H.; He, M.; Song, B. Enhanced electrical conductivity and lithium ion diffusion rate of LiFePO4 by Fe site and P site doping. *AIP Adv.* **2023**, 13. [CrossRef]
59. Lee, S.B.; Cho, S.H.; Aravindan, V.; Kim, H.S.; Lee, Y.S. Improved Cycle Performance of Sulfur-Doped $LiFePO_4$ Material at High Temperatures. *Bull. Korean Chem. Soc.* **2009**, *30*, 2223–2226.
60. Liao, X.Z.; He, Y.S.; Ma, Z.F.; Zhang, X.M.; Wang, L. Effects of fluorine-substitution on the electrochemical behavior of $LiFePO_4$/C cathode materials. *J. Power Sources* **2007**, *174*, 720–725. [CrossRef]
61. Mi, Y.Y.; Yang, C.K.; Zuo, Z.C.; Qi, L.Y.; Tang, C.X.; Zhang, W.D.; Zhou, H.H. Positive Effect of Minor Manganese Doping on the Electrochemical Performance of $LiFePO_4$/C under Extreme Conditions. *Electrochim. Acta* **2015**, *176*, 642–648. [CrossRef]
62. Wang, Y.; Zhang, J.; Xue, J.; Ke, X.; Liang, G. $LiFePO_4$/C composites with high compaction density as cathode materials for lithium-ion batteries with high volumetric energy density. *Ionics* **2021**, *27*, 4687–4694. [CrossRef]
63. Yang, Y.; Liao, X.Z.; Ma, Z.F.; Wang, B.F.; He, L.; He, Y.S. Superior high-rate cycling performance of $LiFePO_4$/C-PPy composite at 55 °C. *Electrochem. Commun.* **2009**, *11*, 1277–1280.
64. Zhu, S.; Huang, A.; Xu, Y. Improving Methods for better Performance of Commercial $LiFePO_4$/C Batteries. *Int. J. Electrochem. Sci.* **2021**, *16*, 210564.
65. Henschel, J.; Schwarz, J.L.; Glorius, F.; Winter, M.; Nowak, S. Further Insights into Structural Diversity of Phosphorus-Based Decomposition Products in Lithium Ion Battery Electrolytes via Liquid Chromatographic Techniques Hyphenated to Ion Trap-Time-of-Flight Mass Spectrometry. *Anal. Chem.* **2019**, *91*, 3980–3988. [CrossRef] [PubMed]
66. Nishi, Y. Lithium ion secondary batteries; past 10 years and the future. *J. Power Sources* **2001**, *100*, 101–106. [CrossRef]
67. Tarascon, J.M.; Guyomard, D. New electrolyte compositions stable over the 0-V to 5-V voltage range and compatible with the $Li_{1+X}Mn_2O_4$ carbon Li-Ion cells. *Solid State Ion.* **1994**, *69*, 293–305. [CrossRef]
68. Wu, H.C.; Su, C.Y.; Shieh, D.T.; Yang, M.H.; Wu, N.L. Enhanced high-temperature cycle life of $LiFePO_4$-based Li-ion batteries by vinylene carbonate as electrolyte additive. *Electrochem. Solid State Lett.* **2006**, *9*, A537–A541. [CrossRef]
69. Matsumoto, K.; Inoue, K.; Nakahara, K.; Yuge, R.; Noguchi, T.; Utsugi, K. Suppression of aluminum corrosion by using high concentration LiTFSI electrolyte. *J. Power Sources* **2013**, *231*, 234–238. [CrossRef]
70. Myung, S.T.; Natsui, H.; Sun, Y.K.; Yashiro, H. Electrochemical behavior of Al in a non-aqueous alkyl carbonate solution containing LiBOB salt. *J. Power Sources* **2010**, *195*, 8297–8301. [CrossRef]
71. Chen, X.L.; Xu, W.; Engelhard, M.H.; Zheng, J.M.; Zhang, Y.H.; Ding, F.; Qian, J.F.; Zhang, J.G. Mixed salts of LiTFSI and LiBOB for stable $LiFePO_4$-based batteries at elevated temperatures. *J. Mater. Chem. A* **2014**, *2*, 2346–2352. [CrossRef]
72. Li, F.Q.; Gong, Y.; Jia, G.F.; Wang, Q.L.; Peng, Z.J.; Fan, W.; Bai, B. A novel dual-salts of LiTFSI and LiODFB in $LiFePO_4$-based batteries for suppressing aluminum corrosion and improving cycling stability. *J. Power Sources* **2015**, *295*, 47–54. [CrossRef]
73. Liang, W.; Zhang, Y.; Yang, R.; Zhu, Y. A room-temperature ionic liquid-based superionic conductive polymer electrolyte with high thermal stability for long-cycle-life lithium batteries. *Colloid Polym. Sci.* **2022**, *300*, 1281–1289. [CrossRef]
74. Logan, E.R.; Hebecker, H.; Eldesoky, A.; Luscombe, A.; Johnson, M.B.; Dahn, J.R. Performance and Degradation of $LiFePO_4$/Graphite Cells: The Impact of Water Contamination and an Evaluation of Common Electrolyte Additives. *J. Electrochem. Soc.* **2020**, *167*, 130543. [CrossRef]
75. Chai, L.; Qu, Q.; Zhang, L.; Shen, M.Z.; Zhang, L.; Zheng, H. Chitosan, a new and environmental benign electrode binder for use with graphite anode in lithium-ion batteries. *Electrochim. Acta* **2013**, *105*, 378–383. [CrossRef]
76. Xing, J.; Bliznakov, S.; Bonville, L.; Oljaca, M.; Maric, R. A review of nonaqueous electrolytes, binders, and separators for lithium-Ion batteries. *Electrochem. Energy Rev.* **2022**, *5*, 14. [CrossRef]
77. Courtemanche, R.J.M.; Pinter, T.; Hof, F. Just add tetrazole: 5-(2-pyrrolo)tetrazoles are simple, highly potent anion recognition elements. *Chem. Commun.* **2011**, *47*, 12688–12690. [CrossRef]

78. Kuenzel, M.; Choi, H.; Wu, F.; Kazzazi, A.; Axmann, P.; Wohlfahrt-Mehrens, M.; Bresser, D.; Passerini, S. Co-Crosslinked Water-Soluble Biopolymers as a Binder for High-Voltage $LiNi_{0.5}Mn_{1.5}O_4$Graphite Lithium-Ion Full Cells. *ChemSusChem* **2020**, *13*, 2650–2660. [CrossRef] [PubMed]
79. Ding, L.; Leones, R.; Omar, A.; Guo, J.; Lu, Q.; Oswald, S.; Nielsch, K.; Giebeler, L.; Mikhailova, D. Highly Efficient Multicomponent Gel Biopolymer Binder Enables Ultrafast Cycling and Applicability in Diverse Battery Formats. *ACS Appl. Mater. Interfaces* **2020**, *12*, 53827–53840. [CrossRef] [PubMed]
80. Ding, L.; Leones, R.; Schmeida, T.; Nielsch, K.; Mikhailova, D. Superior high-temperature rate performance of $LiFePO_4$ cathode: The stabilizing effect of a multicomponent gel biopolymer binder. *J. Power Sources* **2022**, *521*, 230955. [CrossRef]
81. Liu, Z.; Jiang, Y.; Hu, Q.; Guo, S.; Yu, L.; Li, Q.; Liu, Q.; Hu, X. Safer Lithium-Ion Batteries from the Separator Aspect: Development and Future Perspectives. *Energy Environ. Mater.* **2021**, *4*, 336–362. [CrossRef]
82. Shi, H.; Fu, Z.; Xu, W.; Xu, N.; He, X.; Li, Q.; Sun, J.; Jiang, R.; Lei, Z.; Liu, Z.-H. Dual-Modified Electrospun Fiber Membrane as Separator with Excellent Safety Performance and High Operating Temperature for Lithium-Ion Batteries. *Small* **2024**, *20*, 2309896. [CrossRef] [PubMed]
83. Cho, K.; Balamurugan, C.; Im, H.; Kim, H.-J. Ceramic-coated separator to enhance cycling performance of lithium-ion batteries at high current density. *Korean J. Met. Mater.* **2021**, *59*, 813–820. [CrossRef]
84. Shi, C.; Dai, J.; Shen, X.; Peng, L.; Li, C.; Wang, X.; Zhang, P.; Zhao, J. A high-temperature stable ceramic-coated separator prepared with polyimide binder/Al_2O_3 particles for lithium-ion batteries. *J. Membr. Sci.* **2016**, *517*, 91–99. [CrossRef]
85. Gao, M.; Zeng, J.; Liang, K.; Zhao, D.; Kong, B. Interfacial assembly of mesoporous silica-based optical heterostructures for sensing applications. *Adv. Funct. Mater.* **2020**, *30*, 1906950. [CrossRef]
86. Jing, P.; Liu, M.; Wang, P.; Yang, J.; Tang, M.; He, C.; Pu, Y.; Liu, M. Flexible nonwoven ZrO_2 ceramic membrane as an electrochemically stable and flame-resistant separator for high-power rechargeable batteries. *Chem. Eng. J.* **2020**, *388*, 124259. [CrossRef]
87. Wang, J.; Liu, Y.; Cai, Q.; Dong, A.; Yang, D.; Zhao, D. Hierarchically Porous Silica Membrane as Separator for High-Performance Lithium-Ion Batteries. *Adv. Mater.* **2022**, *34*, 2107957. [CrossRef] [PubMed]
88. Hao, H.; Tan, R.; Ye, C.; Low, C.T.J. Carbon-coated current collectors in lithium-ion batteries and supercapacitors: Materials, manufacture and applications. *Carbon Energy* **2024**, *6*, e604. [CrossRef]
89. Fu, Y.; Zhu, J.; Hu, C.; Wu, X.; Wang, X. Covalently coupled hybrid of graphitic carbon nitride with reduced graphene oxide as a superior performance lithium-ion battery anode. *Nanoscale* **2014**, *6*, 12555–12564. [CrossRef]
90. Jiang, J.C.; Shi, W.; Zheng, J.M.; Zuo, P.J.; Xiao, J.; Chen, X.L.; Xu, W.; Zhang, J.G. Optimized Operating Range for Large-Format $LiFePO_4$/Graphite Batteries. *J. Electrochem. Soc.* **2014**, *161*, A336–A341. [CrossRef]
91. Sarasketa-Zabala, E.; Gandiaga, I.; Martinez-Laserna, E.; Rodriguez-Martinez, L.M.; Villarreal, I. Cycle ageing analysis of a $LiFePO_4$/graphite cell with dynamic model validations: Towards realistic lifetime predictions. *J. Power Sources* **2015**, *275*, 573–587. [CrossRef]
92. Lewerenz, M.; Münnix, J.; Schmalstieg, J.; Käbitz, S.; Knips, M.; Sauer, D.U. Systematic aging of commercial $LiFePO_4$/Graphite cylindrical cells including a theory explaining rise of capacity during aging. *J. Power Sources* **2017**, *345*, 254–263. [CrossRef]
93. Molaeimanesh, G.R.; Mousavi-Khoshdel, S.M.; Nemati, A.B. Experimental analysis of commercial $LiFePO_4$ battery life span used in electric vehicle under extremely cold and hot thermal conditions. *J. Therm. Anal. Calorim.* **2021**, *143*, 3137–3146. [CrossRef]
94. Jia, Z.; Jin, K.; Mei, W.; Qin, P.; Jinhua, S.; Wang, Q. Advances and perspectives in fire safety of lithium-ion battery energy storage systems. *eTransportation* **2025**, *24*, 100390. [CrossRef]
95. Gao, F.; Fan, M.; Wang, C.; Liu, W.; Zhu, Y. Study on temperature change of $LiFePO_4$/C battery thermal runaway under overcharge condition. *IOP Conf. Ser. Earth Environ. Sci.* **2021**, *631*, 012114. [CrossRef]
96. Bree, G.; Hao, H.; Stoeva, Z.; John Low, C.T. Monitoring state of charge and volume expansion in lithium-ion batteries: An approach using surface mounted thin-film graphene sensors. *RSC Adv.* **2023**, *13*, 7045–7054. [CrossRef]
97. Zhou, X.; Wang, N.; Xu, J.; Zhao, M.; Zhang, C. Research status of management technology and safety protection technology of lithium iron phosphate battery. *Therm. Power Gener.* **2021**, *50*, 9–17.
98. Li, K.; Li, J.; Gao, X.; Lu, Y.; Wang, D.; Zhang, W.; Wu, W.; Han, X.; Cao, Y.-C.; Lu, L.; et al. Effect of preload forces on multidimensional signal dynamic behaviours for battery early safety warning. *J. Energy Chem.* **2024**, *92*, 484–498. [CrossRef]
99. Li, K.; Chen, L.; Gao, X.; Lu, Y.; Wang, D.; Zhang, W.; Wu, W.; Han, X.; Cao, Y.-C.; Wen, J.; et al. Implementing expansion force-based early warning in $LiFePO_4$ batteries with various states of charge under thermal abuse scenarios. *Appl. Energy* **2024**, *362*, 122998. [CrossRef]
100. He, Q.; Yu, B.; Li, Z.; Zhao, Y. Density Functional Theory for Battery Materials. *Energy Environ. Mater.* **2019**, *2*, 264–279. [CrossRef]
101. Tian, X.; Zhou, S.; Hao, H.; Ruan, H.; Gaddam, R.R.; Dutta, R.C.; Zhu, T.; Wang, H.; Wu, B.; Brandon, N.P.; et al. Machine Learning and Density Functional Theory for Catalyst and Process Design in Hydrogen Production. *CHAIN* **2024**, *1*, 150–166. [CrossRef]
102. Nozarijouybari, Z.; Fathy, H.K. Machine learning for battery systems applications: Progress, challenges, and opportunities. *J. Power Sources* **2024**, *601*, 234272. [CrossRef]

103. Lv, C.; Zhou, X.; Zhong, L.; Yan, C.; Srinivasan, M.; Seh, Z.W.; Liu, C.; Pan, H.; Li, S.; Wen, Y.; et al. Machine Learning: An Advanced Platform for Materials Development and State Prediction in Lithium-Ion Batteries. *Adv. Mater.* **2022**, *34*, 2101474. [CrossRef] [PubMed]
104. Xiang, J. A Review of Machine Learning Classification Based on Random Forest Algorithm. *Artif. Intell. Robot. Res.* **2024**, *13*, 143–152.